Journal of Neonatal Surgery
ISSN(Online): 2226-0439
Vol. 14, Issue 32s (2025)
https://www.jneonatalsurg.com

OPEN ACCESS

Cilostazol in Pulmonary Fibrosis: A Molecular Docking Approach to Target Protein discovery

Pranaya Misar[*1], Dr. Kishor Otari[2]

[*1]Research Scholar, Dr. Babasaheb Ambedkar Technological University, Lonere, Raigad 402103, Assistant Professor, N.N. Sattha College of Pharmacy, Ahmednagar 414003.

[2]Principal, Navsahyadri College of Pharmacy**,** Nasrapur, Pune Maharashtra 412213.

[*]**Corresponding author:**

Pranaya Misar

Cite this paper as: Pranaya Misar, Dr. Kishor Otari, (2025) Cilostazol in Pulmonary Fibrosis: A Molecular Docking Approach to Target Protein discovery. *Journal of Neonatal Surgery*, 14 (32s), 2022-2030.

ABSTRACT

Pulmonary fibrosis (PF) is a chronic, progressive, and often fatal interstitial lung disease characterized by excessive extracellular matrix deposition, leading to irreversible lung damage and respiratory failure. Despite recent therapeutic advancements, effective treatments remain limited, highlighting an urgent need for novel pharmacological interventions. Cilostazol, a phosphodiesterase-3 (PDE3) inhibitor, exhibits diverse pharmacological properties, including anti-inflammatory, anti-platelet, and vasodilatory effects, and has shown promise in various fibrotic conditions. This study aimed to computationally identify potential target proteins of cilostazol relevant to the pathogenesis of pulmonary fibrosis using molecular docking simulations. A comprehensive library of known PF-related proteins was curated, and molecular docking was performed between cilostazol and these proteins using AutoDock Vina. Analysis of binding affinities and interaction patterns revealed several promising protein targets. We identify 5 potential therapeutic targets of cilostazol by molecular docking i.e., MMP7, TGF-β R1, Smad3, Wnt3a, GSK-3β and validate the results by evaluating its protective effect against pulmonary fibrosis. These findings suggest that cilostazol may exert its anti-fibrotic effects through multi-targeted mechanisms beyond its classical PDE3 inhibition, potentially modulating key signaling cascades involved in fibroblast activation, collagen synthesis, and inflammatory responses. This *in silico* investigation provides a foundational understanding of cilostazol's potential molecular targets in PF, paving the way for further *in vitro* and *in vivo* validation studies and its potential repurposing as a therapeutic agent for this devastating disease.

1. INTRODUCTION

Pulmonary fibrosis (PF) represents a heterogeneous group of chronic and progressive lung diseases characterized by the relentless accumulation of extracellular matrix (ECM) components, primarily collagen, within the lung parenchyma(1). This pathological process leads to the distortion of lung architecture, impaired gas exchange, and ultimately, respiratory insufficiency and premature death. Idiopathic pulmonary fibrosis (IPF), the most common and severe form, has a median survival of 3-5 years post-diagnosis, underscoring its significant morbidity and mortality burden worldwide (2,3,4). The exact etiology of PF remains elusive, but it is believed to involve a complex interplay of genetic predispositions, environmental factors, and aberrant wound healing responses, leading to persistent activation of fibroblasts into myofibroblasts, which are the primary drivers of ECM production (5).

Current pharmacological treatments for IPF, such as pirfenidone and nintedanib, have demonstrated efficacy in slowing disease progression and preserving lung function, but they do not halt or reverse the fibrotic process, and many patients still experience progressive decline and significant side effects (6). This highlights a critical unmet medical need for more effective, well-tolerated, and potentially curative therapeutic strategies. The complex multifactorial nature of PF pathogenesis suggests that targeting multiple pathways simultaneously might be a more effective approach than single-target therapies (7,8).

Cilostazol (6-[4-(1-cyclohexyl-1H-tetrazol-5-yl)butoxy]-3,4-dihydro-2(1H)-quinolinone) is a quinolinone derivative primarily known as a selective phosphodiesterase-3 (PDE3) inhibitor. Its established clinical utility lies in the treatment of intermittent claudication due to peripheral artery disease, where it exerts vasodilatory and anti-platelet effects(9,10,11). Beyond these well-characterized actions, cilostazol has been shown to possess a spectrum of pleiotropic effects, including anti-inflammatory, anti-proliferative, and anti-oxidative properties (12,13). Emerging evidence from preclinical studies suggests its potential therapeutic benefits in various fibrotic disorders, including liver fibrosis, kidney fibrosis, and cardiac

fibrosis, by modulating key cellular processes involved in fibrogenesis(14). These observations provide a compelling rationale for exploring cilostazol's therapeutic potential in pulmonary fibrosis.

Molecular docking is a computational technique widely employed in drug discovery and development to predict the preferred orientation of a ligand (e.g., a drug molecule) when bound to a macromolecular target (e.g., a protein). This method allows for the estimation of binding affinity and the identification of key intermolecular interactions, thereby providing insights into the potential mechanism of action of a compound and facilitating the identification of novel therapeutic targets. Given the complex nature of pulmonary fibrosis, an *in silico* approach like molecular docking can efficiently screen potential interactions between cilostazol and a multitude of proteins implicated in fibrotic pathways, thereby accelerating the drug repurposing process(15).

In this study, we aimed to systematically investigate the potential molecular targets of cilostazol in the context of pulmonary fibrosis using advanced molecular docking simulations. By identifying the key proteins with which cilostazol interacts and their respective binding affinities, we sought to elucidate the putative mechanisms through which cilostazol might exert its anti-fibrotic effects. The findings from this *in silico* analysis are expected to provide valuable insights into the multifaceted actions of cilostazol and guide future experimental validation, ultimately contributing to the development of novel therapeutic strategies for pulmonary fibrosis.

2. METHODOLOGY

Molecular Docking Studies

Ligand Preparation and Optimization:

We downloaded ligand Cilostazol from database PubChem (https://pubchem.ncbi.nlm.nih.gov) and optimized our compound using the software MarvinSketch (ChemAxon, Version 22.13). Hydrogens were added and cleaned up each structure in 2D and 3D, both dimensional perspectives. We generated several possible molecule conformers and chose the lowest energy configuration for additional analysis. We used the DockPrep module in Chimera version 1.17.1 (build 42449) to process our Mol2 files of the 3D structures. Then, we ran the process using default parameters like protonation states with AM1-BCC during conjugate gradient optimization.

Protein Preparation:

The RCSB Protein Data Bank(16) (https://www.rcsb.org/) offered us the crystal structure of with MMp7, TGF-β R1, Smad3, Wnt3a, GSK-3β with PDB ID 7WXX, 6B8Y, 1U7F, 4A0P and 4J1R respectively. The selected protein was validated by examining protein resolution and wwPDB scores, observing missing residues in binding sites on PDB sum (17) (https://www.ebi.ac.uk/thornton-srv/databases/pdbsum/), and looking at Ramachandran plot data. We optimized the raw PDB file using the Dock Prep module on Chimera by removing unwanted residues and adding hydrogen atoms to prepare the structure for the AMBER force field and charge adjustment. We exported our refined structure to PDB file format. We used AutoDock Tools version 1.5.6, developed by The Scripps Research Institute, to convert our protein structure to the PDBQT format

Grid Parameters:

The molecular docking studies were carried out using AutoDockTools 1.5.6 (18), Chimera (19), and Maestro (20) were employed for grid Generation and validation. The grid parameters were obtained by using CASTp 3.0: Computed Atlas of Surface Topography of proteins server (http://sts.bioe.uic.edu/castp/index.html?2r7g), with a grid point spacing of 0.375 Å. Table.1. Illustrated the grid parameters of identified protein. The size of Grid box was made small so that it should be consistent with protein's active site and with the ligand expected to be docked.

Sr.no	PDB/UniProt Id	Centre Coordinates			Size Coordinates		
		x	y	z	x	y	z
1	**7WXX**	-26.207	-22.4875	-4.9172	20	20	20
2	**6B8Y**	5.32	8.88	5.09	20	20	20
3	**1U7F**	-6.5054	57.7798	86.5822	20	20	20
4	**4A0P**	50.237	46.9186	16.5556	20	20	20
5	**4J1R**	37.29	32.47	30.9	20	20	20

Table 1. **Grid Parameters of Identified target proteins**

Molecular Docking Simulation:

Our docking simulations used AutoDock Vina(21,22)Version 1.2.5 through a Windows operating system. We ran the procedure triplicate using different grid sizes to verify reliability and repeatability. Our software operated based on preset conditions that handled CPU speed, grid size, search intensity, mode quantity, and energy limits. Post-Docking Analysis: We used Python scripts created from AutoDockTools features to process the docking results. Our scripts enabled us to split and form protein and ligand connections. We studied protein-ligand structures through Discovery Studio(23), PLIP (24) (https://plip-tool.biotec.tu-dresden.de/plip-web/plip/index), and MAESTRO visualization programs.

Validation Parameters:

Table 2 and Fig.1.showed the validation parameters and Ramchandran Plot obtained from PROCHECK.

PARAMETERS	Details					STANDARDS
Method of experiment	X-ray Diffraction					
Protein Id	7WXX	6B8Y	1U7F	4A0P	4J1R	
Mutation	Yes			No		
Resolution	1.5 Å	1.65 Å	2.6 Å	1.9 Å	2.70 Å	Near about 3.00 Å
wwPDB Validation	Better					
Co-Crystal Ligand	Absent	D0A	Absent	Absent	I5R	
Ramchandran Plot (by PROCHECK server) Residues in favored + Allowed regions	100%					>88 %

Table2: Comparison between standard values and retrieved protein from RCSB Protein Bank Database for validation of protein Selected for docking study

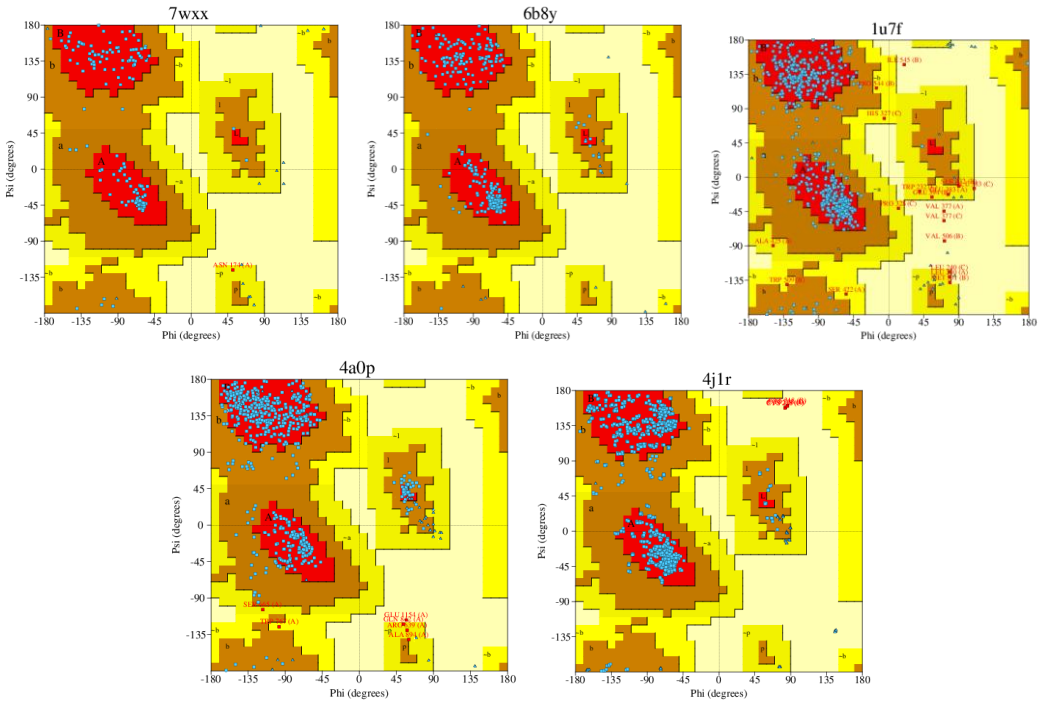

Figure1: Ramachandran Plot 7WXX, 6B8Y, 1U7F, 4A0P and 4J1R obtained from PROCHECK

PDB/ UniProt ID	Active sites amino acids
7WXX	LEU176A, ILE206A, TYR210A, ALA211A, HIS214A, GLN215A, PRO234A, TYR236B
6B8Y	LYS232A, HIS283A, ASP351A, ILE211A, VAL219A, ALA230A, GLU245A, TYR249A, LEU260A, PHE262A, LEU278A, VAL279A, SER280A, ASP281A, TYR282A, GLY286A, LYS337A, ASN338A, LEU340A
1U7F	GLN242A, ARG243A, VAL244A, GLY245A, GLU246A, THR247A, PHE248A, HIS249A, PRO263A, ASN265A, SER266A, ARG268A, PHE269A, CYS270A, LEU273A, LEU274A, SER275A, ASN276A, VAL277B, GLY337C, SER234C, SER236C, TYR238C, ARG243C, GLY245C, THR247C, HIS249C, GLU397C, HIS399C, ASN401C
4A0P	ASP1018A, LEU1019A, SER1020A, ILE1021A, ILE1023A, TYR1024A, VAL1062A, VAL1063A, VAL1064A, PRO1066A, GLU1067A, ALA1106A, LEU1107A, ALA1108A, LEU1109A, ASP1110A, SER1111A, GLY1149A, LEU1150A, THR1151A, VAL1152A, ILE1190A, ILE1191A, HIS1192A, ALA1193A, VAL1194A, LYS1195A, GLU1196A, LEU1197A, ASN1198A, TYR1202A, ILE970A, ASP971A, TYR972A, PRO974A
4J1R	ASP744A, ILE198A, GLY204A, PHE235A, VAL251A, VAL252A, VAL253A, , , TYR757A, VAL761A, VAL763A, VAL764A, PRO768A, LEU1218A, CYS1299A, CYS1300A, ASP1306A, ASP1307A

Table3: Active sites amino acids for identified target proteins in pulmonary fibrosis.

VISUALIZATION:

Protein-ligand complexes were visualized using Biovia Discovery Studio visualizer and Maestro 12.3 (academic edition) for 2D and 3D interactions.

RESULTs:

The results of molecular interactions retrieved from the molecular docking were demonstrated in Table.4 and 5. which, illustrated that the system was successfully validated as the predicted and crystallographic molecular poses closely corelated, with an RMSD (root mean square deviation) of less than 2 Å.; the test compound cilostazol exhibited the binding free energy comparable to the experimental ligand. In certain cases, cilostazol showed even greater binding efficacy than the crystallographic ligand. The test compound cilostazol exhibits comparable binding affinities to experimental inhibitors suggesting its potential to target these same proteins which may result in reducing progression of pulmonary fibrosis. Figure 2,3,4,5 and 6 showed the interactions of cilostazol and identified target proteins.

Sr No	Name of the Target	PDBID	Co crystallized ligand	Reference RMSD	Binding free energy (Cocrystallized ligand)	Binding free energy (Cilostazol)
1	MMP7	7WXX	absent	-	-	-7.719
2	TGF-β1	6B8Y	D0A	1.25	-11.326	-9.31
3	Smad3	1U7F	absent	-	-	-8.09
4	Wnt3a	4A0P	absent	-	-	-8.631
5	GSK-3β	4J1R	I5R	1.49	-8.549	-7.683

Table4: Binding energies of ligands

PDB/UniProt ID	Name of molecules	Binding energy	type of interaction	residue ID	Distance
7WXX	Cilostazol	-7.719	Hydrophobic Interactions	ALA211A	3.72
				HIS214A	3.76
				TYR236A	3.42
				TYR236A	3.86
			Hydrogen Bonds	LEU176A	2.24
				ALA177A	2.34
				ALA179A	1.91
				GLN215A	2.99
				GLN215A	3.12
			p-Stacking	HIS224A	4.79
6B8Y		-9.31	Hydrophobic Interactions	VAL219A	3.85
				ALA230A	3.55
				LYS232A	3.63
				TYR249A	3.33
				PHE262A	3.88
				LEU278A	3.24
				LEU340A	3.82
				LEU340A	3.47
			Hydrogen Bonds	LYS232A	2.04
				LYS337A	2.65
				ASP351A	2.62
			p-Cation Interactions	LYS232A	3.32
	D0A	-11.326	Hydrophobic Interactions	ALA230A	3.7
				LYS232A	3.67
				LEU278A	3.7
				LEU340A	3.63
				LEU340A	3.71
			Hydrogen Bonds	LYS232A	2.52
				SER280A	3.14
				HIS283A	2.27
				ASP351A	2.29
1U7F	Cilostazol	-8.09	Hydrophobic Interactions	PHE231C	4
				PHE248A	3.64
				PRO263A	3.95
				PHE269A	3.99
				PHE269A	3.63
				LEU273A	3.71
			Hydrogen Bonds	SERSER	2.77
				HIS399C	2.78

				ASN401C	2.12
			p-Stacking	HIS249C	4.29
4A0P		-8.631	Hydrophobic Interactions	PRO974A	3.84
				ILE1023A	3.88
				ILE1023A	3.77
				VAL1063A	3.5
				ALA1193A	3.73
				VAL1194A	3.82
				LYS1195A	3.46
			Hydrogen Bonds	HIS1192A	3.38
				ALA1193A	3.33
				LYS1195A	3.35
4J1R		-7.683	Hydrophobic Interactions	PHE67A	3.9
				VAL70A	3.49
				ALA83A	3.81
				LYS85A	3.6
				TYR134A	3.81
				LEU188A	3.66
				ASP200A	3.81
			Hydrogen Bonds	ASP200A	2.83
				GLN185A	2.47
				THR138A	2.62
	I5R	-8.549	Hydrophobic Interactions	PHE67A	3.64
				VAL70A	3.59
				LEU132A	3.96
				LEU188A	3.81
			Hydrogen Bonds	ASP133A	2.04
				VAL135A	2.47
				ASP200A	2.79

Table5: Docking Score and intermolecular interactions of ligands with 7WXX, 6B8Y, 1U7F, 4A0P and 4J1R from PLIP.

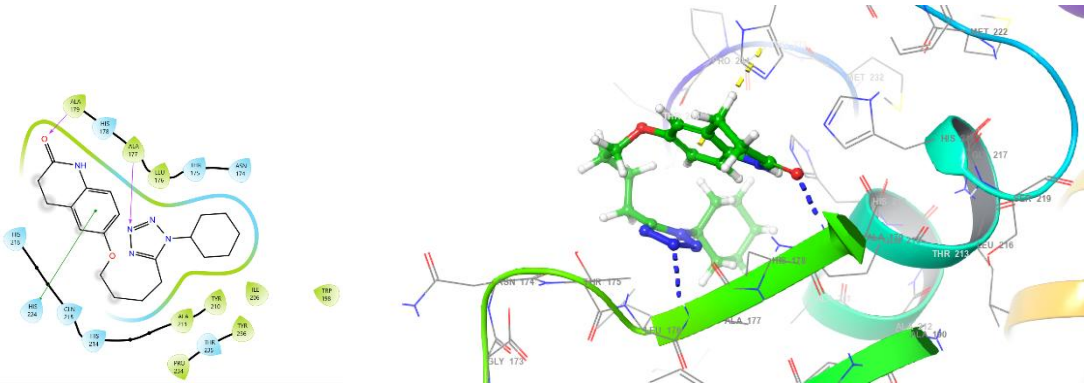

Fig 2: 2D and 3D images of the interaction of protein 7WXX with Cilostazol.

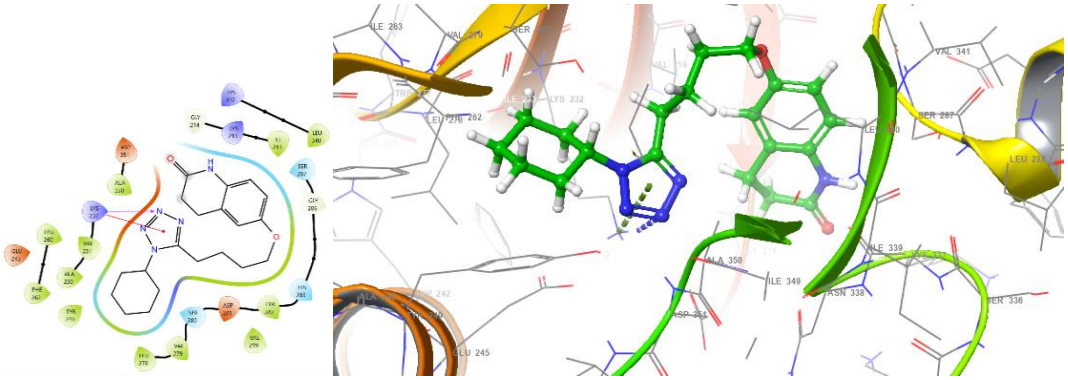

Fig 3: 2D and 3D images of the interaction of protein 6B8Y with Cilostazol.

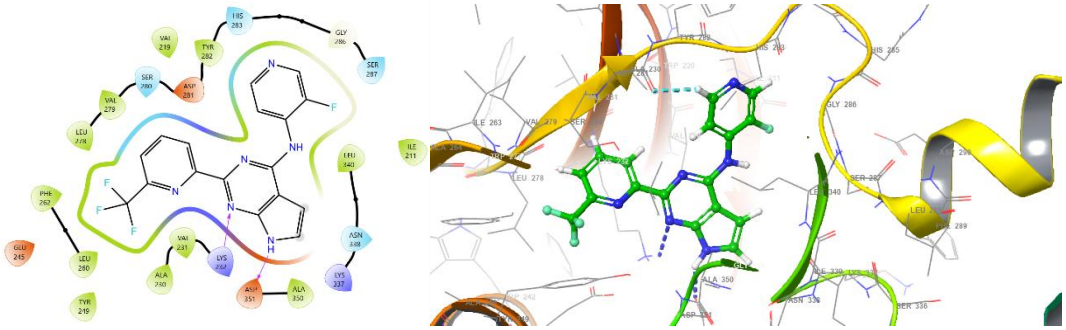

Fig 4: 2D and 3D images of the interaction of protein 6B8Y with D0A.

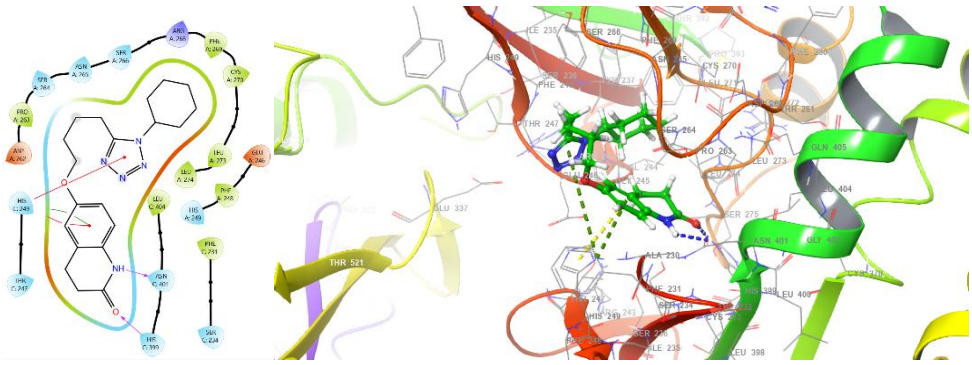

Fig 5: 2D and 3D images of the interaction of protein 1U7F with Cilostazol.

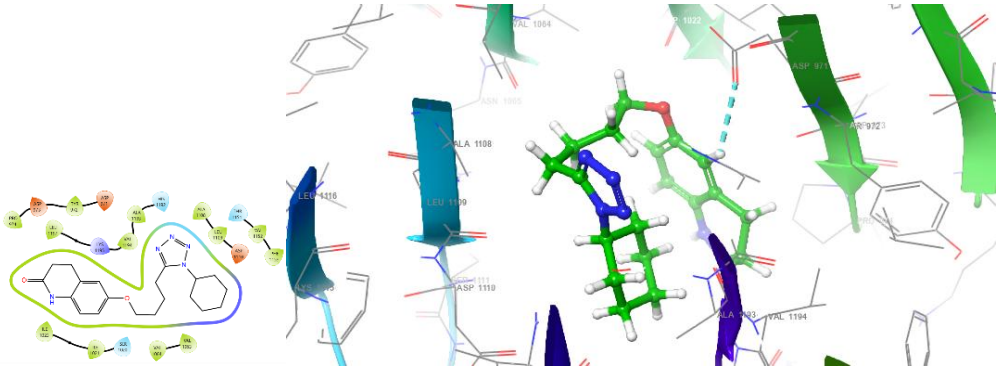

Fig 6: 2D and 3D images of the interaction of protein 4A0P with Cilostazol.

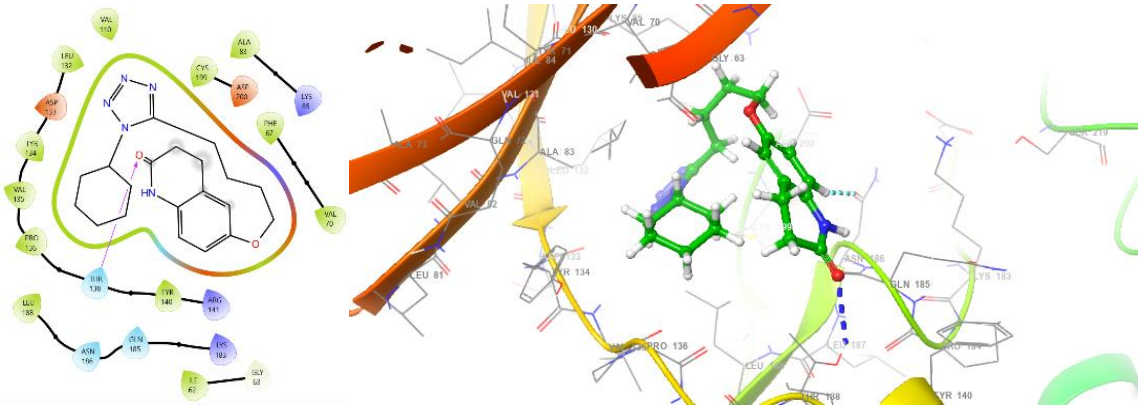

Fig 7: 2D and 3D images of the interaction of protein 4J1Rwith Cilostazol.

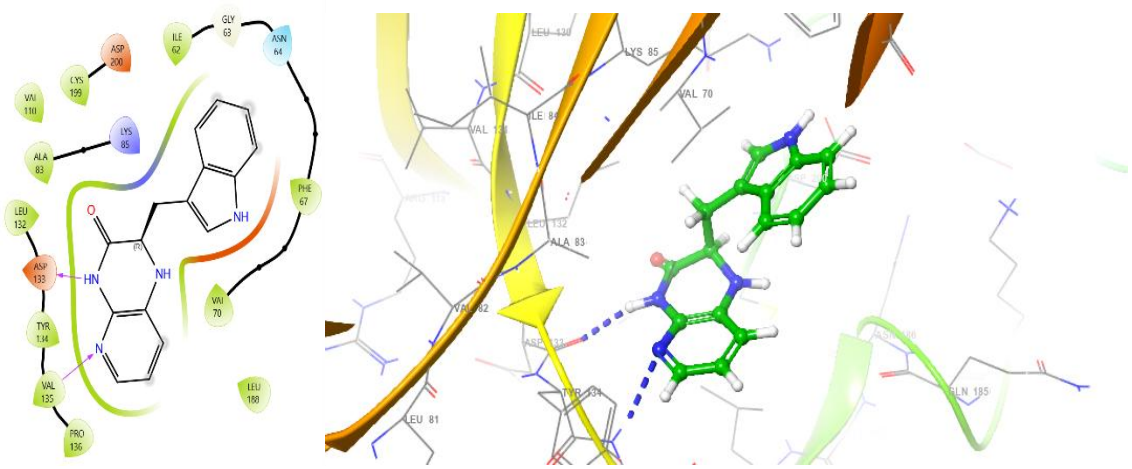

Fig: 2D and 3D images of the interaction of protein 4J1Rwith I5R.

3. CONCLUSION

This study utilized molecular docking simulations to identify potential therapeutic targets of cilostazol in pulmonary fibrosis (PF). The in silico investigation successfully identified five promising protein targets: MMP7, TGF-β R1, Smad3, Wnt3a, and GSK-3β. These findings suggest that cilostazol's protective effects against PF may stem from multi-targeted mechanisms, extending beyond its known PDE3 inhibition. By potentially modulating key signaling pathways involved in fibroblast activation, collagen synthesis, and inflammatory responses, cilostazol demonstrates promise as a multifaceted anti-fibrotic agent. This computational study provides a crucial foundation for future *in vitro* and *in vivo* validation, supporting the potential repurposing of cilostazol as a therapeutic intervention for pulmonary fibrosis.

REFERENCES

[1] Zhai K, Zang D, Yang S, Zhang Y, Niu S, Yu X. Biomarkers for Early Diagnosis of Idiopathic Pulmonary Fibrosis: A Systematic Review. Journal of Medical and Biological Engineering. 2024 Oct;44(5):666-75.

[2] Tsukioka T, Takemura S, Minamiyama Y, Mizuguchi S, Toda M, Okada S. Attenuation of Bleomycin-induced pulmonary fibrosis in rats with S-Allyl cysteine. Molecules. 2017 Mar 29;22(4):543.

[3] Wang Z, Li X, Chen H, Han L, Ji X, Wang Q, Wei L, Miu Y, Wang J, Mao J, Zhang Z. Resveratrol alleviates bleomycin-induced pulmonary fibrosis via suppressing HIF-1α and NF-κB expression. Aging (Albany NY). 2021 Jan 20;13(3):4605.

[4] Liu H, Heenan KM, Coyle L, Chaudhuri N. Progressive pulmonary fibrosis: a need for real world data to solve real world clinical problems. BMJ medicine. 2024 Aug 16;3(1):e000911.

[5] Sofia C, Comes A, Sgalla G, Richeldi L. Promising advances in treatments for the management of idiopathic pulmonary fibrosis. Expert Opinion on Pharmacotherapy. 2024 Apr 12;25(6):717-25.

[6] Alzahrani B, Gaballa MM, Tantawy AA, Moussa MA, Shoulah SA, Elshafae SM. Blocking Toll-like receptor 9 attenuates bleomycin-induced pulmonary injury. Journal of Pathology and Translational Medicine. 2022 Mar 2;56(2):81-91.

[7] Zheng M, Zhu W, Gao F, Zhuo Y, Zheng M, Wu G, Feng C. Novel inhalation therapy in pulmonary fibrosis: principles, applications and prospects. Journal of Nanobiotechnology. 2024 Mar 29;22(1):136.

[8] Huang G, Yang X, Yu Q, Luo Q, Ju C, Zhang B, Chen Y, Liang Z, Xia S, Wang X, Xiang D. Overexpression of STX11 alleviates pulmonary fibrosis by inhibiting fibroblast activation via the PI3K/AKT/mTOR pathway. Signal Transduction and Targeted Therapy. 2024 Nov 11;9(1):306.

[9] Hada Y, Uchida HA, Umebayashi R, Yoshida M, Wada J. Cilostazol attenuates AngII-induced cardiac fibrosis in apoE deficient mice. International journal of molecular sciences. 2022 Aug 13;23(16):9065.

[10] Motta NA, Autran LJ, Brazao SC, de Oliveira Lopes R, Scaramello CB, Lima GF, de Brito FC. Could cilostazol be beneficial in COVID-19 treatment? Thinking about phosphodiesterase-3 as a therapeutic target. International immunopharmacology. 2021 Mar 1;92:107336.

[11] Kherallah RY, Khawaja M, Olson M, Angiolillo D, Birnbaum Y. Cilostazol: a review of basic mechanisms and clinical uses. Cardiovascular drugs and therapy. 2022 Aug 1:1-6.

[12] Kabil SL. Beneficial effects of cilostazol on liver injury induced by common bile duct ligation in rats: role of SIRT 1 signaling pathway. Clinical and experimental pharmacology and physiology. 2018 Dec;45(12):1341-50.

[13] Saito S, Hata K, Iwaisako K, Yanagida A, Takeiri M, Tanaka H, Kageyama S, Hirao H, Ikeda K, Asagiri M, Uemoto S. Cilostazol attenuates hepatic stellate cell activation and protects mice against carbon tetrachloride-induced liver fibrosis. Hepatology research. 2014 Apr;44(4):460-73.

[14] Han K, Zhang Y, Yang Z. Cilostazol protects rats against alcohol-induced hepatic fibrosis via suppression of TGF-β1/CTGF activation and the cAMP/Epac1 pathway. Experimental and Therapeutic Medicine. 2019 Mar 1;17(3):2381-8.

[15] Li J, Wang Y, Wang R, Wu MY, Shan J, Zhang YC, Xu HM. Study on the molecular mechanisms of tetrandrine against pulmonary fibrosis based on network pharmacology, molecular docking and experimental verification. Heliyon. 2022 Aug 1;8(8).

[16] Berman, H.M., Westbrook, J., Feng, Z., Gilliland, G., Bhat, T.N., Weissig, H., Shindyalov, I.N. and Bourne, P.E., 2000. The protein data bank. Nucleic acids research, 28(1), pp.235-242.

[17] Laskowski, R.A., Hutchinson, E.G., Michie, A.D., Wallace, A.C., Jones, M.L. and Thornton, J.M., 1997. PDBsum: a Web-based database of summaries and analyses of all PDB structures. *Trends in biochemical sciences*, *22*(12), pp.488-490.

[18] Morris, G. M., Huey, R., Lindstrom, W., Sanner, M. F., Belew, R. K., Goodsell, D. S. and Olson, A. J. (2009) Autodock4 and AutoDockTools4: automated docking with selective receptor flexiblity. *J. Computational Chemistry* 2009, **16**: 2785-91.

[19] UCSF Chimera--a visualization system for exploratory research and analysis. Pettersen EF, Goddard TD, Huang CC, Couch GS, Greenblatt DM, Meng EC, Ferrin TE. J Comput Chem. 2004 Oct;25(13):1605-12.

[20] Schrödinger Release 2021-1: Maestro, Schrödinger, LLC, New York, NY, 2021.

[21] J. Eberhardt, D. Santos-Martins, A. F. Tillack, and S. Forli AutoDock Vina 1.2.0: New Docking Methods, Expanded Force Field, and Python Bindings, J. Chem. Inf. Model. (2021) DOI 10.1021/acs.jcim.1c00203

[22] O. Trott, A. J. Olson,AutoDock Vina: improving the speed and accuracy of docking with a new scoring function, efficient optimization and multithreading, J. Comp. Chem. (2010) DOI 10.1002/jcc.21334.

[23] BIOVIA, Dassault Systèmes, [Discovery Studio], [2021], San Diego: Dassault Systèmes, [2021].

[24] Salentin, S., Schreiber, S., Haupt, V. J., Adasme, M. F., & Schroeder, M. (2015). PLIP: fully automated protein–ligand interaction profiler. Nucleic acids research, 43(W1), W443-W447.